Biofabrication

PAPER

Double printing of hyaluronic acid/poly(glycidol) hybrid hydrogels with poly(ε-caprolactone) for MSC chondrogenesis

Simone Stichler[1,5], **Thomas Böck**[1,2,5], **Naomi Paxton**[1], **Sarah Bertlein**[1], **Riccardo Levato**[3], **Verena Schill**[1], **Willi Smolan**[1], **Jos Malda**[3,4], **Jörg Teßmar**[1], **Torsten Blunk**[2] and **Jürgen Groll**[1]

[1] Department of Functional Materials in Medicine and Dentistry and Bavarian Polymer Institute, University of Würzburg, Pleicherwall 2, 97070 Würzburg, Germany
[2] Department of Trauma, Hand, Plastic and Reconstructive Surgery, University of Würzburg, Oberdürrbacher Str. 6, 97080 Würzburg, Germany
[3] Department of Orthopaedics, University Medical Center Utrecht, Utrecht University, PO box 85500, 3508 GA Utrecht, The Netherlands
[4] Department of Equine Sciences, Faculty of Veterinary Medicine, Utrecht University. Yalelaan 122, 3584 CM Utrecht, The Netherlands
[5] These authors contributed equally.

E-mail: juergen.groll@fmz.uni-wuerzburg.de

RECEIVED
3 July 2017

REVISED
24 August 2017

ACCEPTED FOR PUBLICATION
14 September 2017

PUBLISHED
14 November 2017

Keywords: bioink, double printing, thiol-ene cross-linking, hyaluronic acid, poly(glycidol), chondrogenic differentiation

Supplementary material for this article is available online

Abstract

This study investigates the use of allyl-functionalized poly(glycidol)s (P(AGE-*co*-G)) as a cytocompatible cross-linker for thiol-functionalized hyaluronic acid (HA-SH) and the optimization of this hybrid hydrogel as bioink for 3D bioprinting. The chemical cross-linking of gels with 10 wt.% overall polymer concentration was achieved by a UV-induced radical thiol-ene coupling between the thiol and allyl groups. The addition of unmodified high molecular weight HA (1.36 MDa) enabled the rheology to be tuned for extrusion-based bioprinting. The incorporation of additional HA resulted in hydrogels with a lower Young's modulus and a higher swelling ratio, especially in the first 24 h, but a comparable equilibrium swelling for all gels after 24 h. Embedding of human and equine mesenchymal stem cells (MSCs) in the gels and subsequent *in vitro* culture showed promising chondrogenic differentiation after 21 d for cells from both origins. Moreover, cells could be printed with these gels, and embedded hMSCs showed good cell survival for at least 21 d in culture. To achieve mechanically stable and robust constructs for the envisioned application in articular cartilage, the formulations were adjusted for double printing with thermoplastic poly(ε-caprolactone) (PCL).

1. Introduction

Bioprinting, a major strategy in biofabrication, is aimed at the direct fabrication of cells together with materials into hierarchical cell-material constructs [1]. Materials that are suitable for this purpose, so called bioinks, are a decisive component of this technology. Hydrogels, mainly based on natural polymers, such as gelatin or alginate, are most prominently used as the basis for bioinks in several biofabrication approaches [2–6]. Synthetic polymers offer the advantages of controlled preparation with better defined molecular weights, pre-determined chemical composition and functionality, which enables the preparation of hydrogels with defined chemical and physical properties. One often applied example is poly(ethylene glycol) (PEG), a linear polyether that is biocompatible and FDA approved. Poly(glycidol)s (PG) are chemically similar but feature additional hydroxyl methylene side groups at each repeating unit, which can be further chemically functionalized, e.g. with carboxylates, allyl and thiol groups [7, 8]. Furthermore, the anionic polymerization of glycidyl ethers with different and orthogonally removable protective groups allow for the preparation of polymers with different functionalities along the PG chain [9]. Previously, we have shown that pure PG bioinks, based on allyl- and thiol-functional polyglycidols and using high molecular weight hyaluronic acid (HA) as a thickener that is not covalently integrated into the network after printing, could be printed with a high shape fidelity and reasonable cellular viability and differentiation [10].

However, PG itself is, similar to PEG, bioinert and does not allow sufficient cell–material interactions, so that the additional bioactivation of PG-based bioinks is necessary to facilitate interaction with cells.

HA is a major component of the natural extracellular matrix (ECM) of many tissues and is already widely used in hydrogels for different biomedical applications [11–15]. Moreover, it is known from the literature that the functional groups of HA can also be chemically modified in many different ways, which makes natural HA suitable for chemical cross-linking approaches [11]. Biologically, HA is an important part of the ECM in cartilage, a tissue without an intrinsic healing capacity for which biofabrication possesses great potential [16, 17]. In the cartilage ECM, HA facilitates cellular attachment and migration by CD44 [18] and CD168 receptors [19], which would provide the missing cell–material interaction to PG-based bioinks. Furthermore, HA is also known to play a significant role in the regulation of stem cell behavior [20], and, especially in the area of cartilage engineering studies, has shown many beneficial effects on the chondrogenic differentiation of mesenchymal stem cells (MSCs) upon exposure to HA-enriched scaffolds [21–23].

In this study, we thus aimed to replace one of the PG components in our previously developed system by chemically functionalizing HA in order to yield a more bioactive and cell friendly bioink, especially with regard to the post-fabrication performance. To enable the bioprinting of mechanically robust scaffolds, we further aimed to double print with thermoplastic biodegradable poly(ε-caprolactone) (PCL), as demonstrated for other hydrogel formulations [24]. We therefore prepared thiol-functionalized HA (HA-SH) and allyl-functional PGs (P(AGE-*co*-G)) and prepared hydrogels via a UV-initiated thiol-ene reaction. As an example of the biological applicability, MSCs from human (hMSC) and equine (eMSC) origin were cultured in the developed hydrogel and the quality of chondrogenesis was assessed. These results showed clear advantages of the hybrid PG-HA gels in comparison to gels composed of PG only. We then optimized the formulation with regard to the rheology for printability, and to demonstrate the printability of the system with good shape fidelity if additional high molecular weight (1.36 MDa) pristine HA is added with 2.5 wt% in the formulation. Double printing with PCL enabled hydrogel solutions to be printed with a lower amount (1 wt.%) of unmodified high molecular weight HA, and cells were vital at least 21 d after printing in this formulation.

2. Materials and methods

2.1. Materials

The allyl glycidyl ether (AGE; $\geqslant$99%, Sigma-Aldrich, St. Louis, MO, USA) and ethoxy ethyl glycidyl ether (EEGE; synthesized as described before [10]) monomers were further purified by drying over calcium hydride (92%, ABCR, Karlsruhe, Germany) and fractionated distillation under reduced pressure. They were subsequently stored under an inert atmosphere.

HA was purchased from BaccaraRose (Alpen, Germany) with two different molecular weights: 27.3 kDa and 1.36 MDa. The low molecular weight HA (27.3 kDa) was used for the functionalization and the high molecular weight HA (1.36 MDa) was used to increase the viscosity for printing the hydrogels.

Chemicals were obtained from Sigma-Aldrich (Sigma-Aldrich, St. Louis, MO, USA), if not stated otherwise.

The primary antibodies were: anti-aggrecan 969D4D11 (Thermo Scientific, Waltham, USA), anti-collagen I ab34710 (Abcam, Cambridge, UK) and anti-collagen II II-4C11 (Acris, Herford, Germany). The secondary antibodies were: donkey anti-mouse (Cy3; Dianova, Hamburg, Germany), goat anti-rabbit (Alexa Fluor 488; Dianova, Hamburg, Germany). αMEM (22561 Gibco, The Netherlands), antibody diluent Dako REAL^{TM} (Dako, Hamburg, Germany), basic fibroblast growth factor (bFGF; BioLegend, London, UK, for eMSCs: R&D Systems, UK)), DAPI mounting medium ImmunoSelect® (Dako, Hamburg, Germany), deuterium oxide (D_2O; Deutero GmbH, Kastellaun, Germany), 3,3′-dithiobis(propanoic dihydrazide) (DTP; Arke Organics, Calcinaia PI, Italy), N-(3-dimethylaminopropyl)-N′-ethylcarbodiimide hydrochloride) (EDC; CarboSynth, Compton, UK), 1,4-dithiothreitol (DTT; AppliChem GmbH, Darmstadt, Germany), Dulbecco's Modified Eagle's Medium/Ham's F-12 (DMEM/F12; Thermo Scientific, Waltham, USA), ethanol (EtOH; 99%, Th. Geyer, Renningen, Germany), fetal bovine serum (FBS; Thermo Scientific, Waltham, USA), FCS (Lonza, The Netherlands), ficoll-paque (GE Healthcare, The Netherlands), hydrochloric acid (HCl; 32%, Merck, Darmstadt, Germany), 2-hydroxy-1-[4-(hydroxyethoxy)-phenyl]-2-methyl-1-propanone (I2959; BASF, Ludwigshafen, Germany), ImmunoSelect® (Dako, Hamburg, Germany), ITS+ Premix (Corning, NY, USA), live/dead cell staining kit (PromoKine, Heidelberg, Germany), papain (Worthington, Lakewood, USA), penicillin–streptomycin (PS; 100 U ml^{-1} penicillin, 0.1 mg ml^{-1} streptomycin; Thermo Scientific, Waltham, USA), phosphate-buffered saline (PBS; Life Technologies, Karlsruhe, Germany), poly(ε-caprolactone) (PCL; Purac Purasorb PC12, Corbion-Purac, Gorinchem, The Netherlands), Proteinase K (DigestAll 4, Life Technologies, Karlsruhe, Germany), tetrahydrofuran (THF; Fisher Scientific, Schwerte, Germany), Tissue Tek® optimal cutting temperature compound (O.C.T.; Sakura Finetek, Tokyo, Japan), transforming growth factor-β1 (TGF-β1; BioLegend, London, UK), trypsin-EDTA (0.25%, Life Technologies, Karlsruhe, Germany) were used as received.

Biotech cellulose ester dialysis membranes (MW cut-off 3500 Da) from spectrumlabs.com (Houston, USA) were used for polymer dialysis.

2.2. Methods

2.2.1. Thiol-functionalized hyaluronic acid (HA-SH) synthesis

HA-SH was synthesized using protocols based on previously described methods [12]. Low molecular weight HA (27.3 kDa, 5.00 g, 12.5 mmol referred to disaccharide units) was dissolved in water (400 ml, Milli-Q) and DTPH (980 mg, 4.11 mmol) was added under continuous stirring. After adjusting the pH of the reaction solution to 4.75 (1 M HCl), EDC (1.31 g, 6.83 mmol) was added to activate the carboxylic acids. The pH was maintained at 4.75 with 1 M HCl and the mixture was stirred overnight. The solution was subsequently degassed with Ar. DTT (1.90 g, 12.3 mmol) was added and the pH was adjusted to 8.5 with 1 M NaOH. After stirring overnight the solution was acidified again (pH 3.5; 1 M HCl) and dialyzed for 24 h against acidified water (pH 3–4, Milli-Q) containing 100 mM NaCl. Then, the polymer was dialyzed against water (Milli-Q) for 48 h and the resulting solution was freeze-dried (Alpha 1–2 LD; Christ, Osterode am Harz, Germany) for 7 d. Finally, thiol-functionalized HA was received with a substitution degree (thiol-functions with the carboxylic acids) of 41% as calculated from the ^{1}H-NMR signals.

^{1}H-NMR (300 MHz, D_2O): $\delta = 4.58$ (bs, 2 H, -CH_2-OH), 4.01-3.39 (m, 10 H, backbone-*H*), 2.94-2.72 (m, 2 H, -CO-CH_2-CH_2-SH), 2.03 (s, 3 H, -NH-C(O)-CH_3) ppm.

GPC: $M_n = 7299$ Da, $M_w = 27\,584$, $Đ = 3.78$.

2.2.2. Poly(allyl glycidyl ether-co-glycidyl) (P(AGE-co-G)) synthesis

The synthesis of linear P(AGE-*co*-G) was carried out as described before [10]. Briefly, an anionic bulk *co*polymerization of AGE (1.50 ml, 12.6 mmol) and EEGE (15.8 ml, 108 mmol) monomers with KO*t*Bu (2.0 ml, 2.00 mmol) as an initiator was conducted at 60 °C for 24 h under an inert atmosphere. The resulting reaction mixture was cooled down to room temperature (RT) and 1 ml EtOH was added to terminate the polymerization. The protected *co*polymer P(AGE-*co*-EEGE) was dissolved in THF (80 ml g^{-1} polymer), and concentrated HCl (2 ml g^{-1} polymer) was added dropwise. After stirring for 4 h, the THF was decanted and the remaining residue was subsequently dissolved in water (10 ml g^{-1} polymer, Milli-Q). This polymer solution was then transferred to dialysis membranes and dialyzed for 3 d against water (2 L, Milli-Q) and finally lyophilized (Alpha 1–2 LD; Christ, Osterode am Harz, Germany). The final *co*polymer P(AGE-*co*-G) was received with a content of allyl-functional monomers of 11%, as proven by ^{1}H-NMR.

^{1}H-NMR (300 MHz, D_2O): $\delta = 6.06$–5.93 (m, 10 H, -O-CH$_2$-C*H*=CH$_2$), 5.41-5.30 (m, 20 H, -O-CH$_2$-CH=C*H*$_2$), 4.13–4.11 (d, 20 H, -O-C*H*$_2$-CH=CH$_2$), 3.84–3.67 (m, 455 H, backbone-*H*), 1.26 (s, 9 H, *t*Bu-*H*) ppm.

GPC: $M_n = 1544$ Da, $M_w = 2955$, $Đ = 1.91$.

2.2.3. Polymer characterization

Both polymers P(AGE-*co*-G) and HA-SH were analyzed via ^{1}H-NMR and GPC measurements. A 300 MHz Bruker Biospin spectrometer (Bruker, Billerica, MA) was used for the ^{1}H-NMR measurements with D_2O as a solvent. The chemical shifts referred to the solvent peak, which was set as an internal reference at $\delta = 4.79$. The allyl-functions of P(AGE-*co*-G) and the thiol-functions of HA-SH, meaning the percentage of allyl and thiol groups, respectively, referring to all monomer or disaccharide units in the backbone, were determined by ^{1}H-NMR. Therefore, the allyl and thiol peaks were set in relation to significant backbone peaks of P(AGE-*co*-G) and HA-SH. respectively.

GPC analysis was realized with a GPC system from Malvern (Herrenberg, Germany) with PEGs as calibration standards (Malvern, Herrenberg, Germany) and deionized water as a solvent (containing 8.5 g L^{-1} $NaNO_3$ and 0.2 g L^{-1} NaN_3). The device is constructed as follows: a column oven (35 °C), a refractive index detector (Viscotek) and Viscotek A-columns A3000 (particle size: 6 μm) and A2000 (particle size: 8 μm). The two columns are made of a porous poly hydroxy-methacrylate polymer and have a length of 300 mm and a width of 8 mm. The samples were measured with an elution rate of 0.7 ml min^{-1}.

2.2.4. MSC isolation and cell culture

The hMSCs were isolated from the surgically removed cancellous bone of patients undergoing hip replacement (the study was approved by the local ethics committee and written informed consent was given by all patients). For the isolation, hMSCs were liberated by extensive washing of bone fragments and bone marrow with PBS. Afterwards, the cell-containing suspension was centrifuged, and the hMSC-containing pellet was resuspended in proliferation medium (DMEM/F12, supplemented with 10% FBS, 1% PS and 5 ng ml^{-1} bFGF) and seeded into T175 cm^2 flasks (Greiner Bio-One, Frickenhausen, Germany). Non-adherent cells were removed by carefully washing with PBS, and adherent cells were subsequently cultured to a sub-confluent level at 37 °C, 5% CO_2 in proliferation medium. The hMSCs were detached with 0.25% trypsin-EDTA, and seeded at a density of approximately 3–5 $\times$ 10^4 cells ml^{-1} into T175 cm^2 flasks. All equine tissue and cells used in this study were obtained from recently deceased equine donors, donated to science by their owners, and according to the guidelines of the Institutional Animal Ethical Committee of the Utrecht University. eMSCs were harvested from

healthy bone marrow in the sternum of skeletally mature equine donors (age 3–10 years old), as previously described [25]. The mononuclear cell fraction was obtained from bone marrow aspirates that were centrifuged for 30 min at 100 g in a Ficoll-paque density gradient. The mononuclear cell fraction was collected, rinsed with PBS and centrifuged a second time at 300 g for 10 min. Afterwards, cells were plated on tissue culture polystyrene and cultured in αMEM supplemented with 0.2 mM L-ascorbic acid 2-phosphate, 10% FCS, 100 units ml^{-1} penicillin with 100 $\mu g\ ml^{-1}$ streptomycin and 1 $ng\ ml^{-1}$ bFGF.

2.2.5. Hydrogel preparation

For the hydrogel preparation, P(AGE-*co*-G) and HA-SH were dissolved in PBS with a total polymer concentration of 10 wt.% (5 wt.% of each polymer, equimolar ratio of SH and allyl groups) and the photoinitiator I2959 (concentration of 0.05 wt.%) was added to the polymer solution. The pH of the slightly acidic hydrogel solutions was neutralized with 5 M NaOH. Afterwards, depending on the experiment cells, hMSCs or eMSCs at passage 3 (amount 20.0×10^6 MSC ml^{-1}) and additional HA (1.36 MDa, concentration of 1 wt.%) were subsequently added to the precursor solution. The hydrogel solution was then pipetted into cylindrical molds (6 mm diameter, 2 or 1 mm height) and cross-linked using UV light (UV hand lamp with filter, A Hartenstein, Wuerzburg, Germany) at 365 nm for 10 min (2 mm height) or 5 min (1 mm height). The intensity of the used UV lamp was 1 mW cm^{-2}.

The MSC-containing hydrogels with a construct size of 6 mm in diameter and 1 mm in height were cultured for 21 d in chondrogenic medium (DMEM high glucose 4.5 g L^{-1}, supplemented with 1% ITS + Premix, 40 $\mu g\ ml^{-1}$ L-proline, 50 $\mu g\ ml^{-1}$ L-ascorbic acid 2-phosphate sesquimagnesium salt hydrate, 0.1 μM dexamethasone, 1 mM sodium pyruvate, 1% PS and 10 $ng\ ml^{-1}$ TGF-β1).

2.2.6. Mechanical testing

To determine the stiffness of the cross-linked hydrogels, triplicates of the two different hydrogel systems (with and without additional 1 wt.% HA) were fabricated as described above with 10 wt.% polymer concentration and a UV irradiation time of 10 min (molds: 6 mm in diameter, 2 mm in height). After incubation at 37 °C for 24 h in 2 ml PBS, the hydrogels were measured using a dynamical mechanical testing machine from Bose (Bose 5500 system, ElectroForce, Eden Prairie, MN, USA) with a load cell of 200 N and 22 N, respectively. The hydrogels were loaded parallel to their long axis and were compressed with a constant cross head displacement rate of 0.001 mm s^{-1}. The Young's modulus of the gels was calculated from the raw data as the slope of the true stress–strain curve in the linear elastic range (0%–10% strain). After mechanical testing the hydrogels were dried to determine their swelling ratio at the time of measurement.

2.2.7. Swelling ratio

The equilibrium swelling ratio (SR) was calculated for the hydrogels after mechanical testing (24 h) using the following equation:

$$SR = \frac{W_s}{W_d} \quad (1)$$

with W_s representing the weight of the swollen hydrogel and W_d the weight of the dried hydrogel after freeze drying.

2.2.8. Swelling study

To determine the swelling kinetics of the different hydrogels, solutions with and without additional HA (1.36 MDa) were prepared. Triplicates of cylindrical constructs (6 mm in diameter, 2 mm in height) were fabricated by adding the two different precursor solutions into molds and cross-linking for 10 min using UV light. The resulting hydrogels were weighed directly after cross-linking (time point 0 h) and subsequently incubated at 37 °C in 2 ml PBS. At specific time intervals (0.5 h, 1 h, 4 h, 7 h, 24 h, 1 w, 2 w, 3 w, 4 w and 5 w) the wet hydrogels were taken out of the solution, blotted dry and weighed again. Subsequently the gels were placed back in fresh PBS buffer after each weighing.

2.2.9. Cell viability assay

The cell viability of the hydrogel-encapsulated MSCs was analyzed using a live/dead cell staining kit. At day 2 and day 21 after cell encapsulation, the hydrogels were washed twice with PBS and incubated in the staining solution (4 μM ethidium homodimer III (EthD-III), 2 μM calcein acetoxymethyl ester (calcein–AM)) for 45 min at RT. Following that, top view images were taken using a fluorescence microscope (Olympus BX51/DP71, Olympus, Hamburg, Germany).

2.2.10. Histological and immunohistochemical analyses

Constructs were fixed in a 3.7% PBS buffered formalin for 60 min at RT, and washed twice in PBS for 15 min prior to incubation in Tissue Tek® O.C.T. overnight at 4 °C. The following day, constructs were shock frozen in liquid nitrogen, and stored at −80 °C [26]. Longitudinal sections (8 μm) were collected on Super Frost® plus glass slides (R Langenbrinck, Emmendingen, Germany) using a cryostat (CM 3050S; Leica, Wetzlar, Germany). For a histological evaluation of the glycosaminoglycan (GAG) deposition, sections were stained with safranin O and fast green, and nuclei were counterstained with Weigert's hematoxylin [27].

For immunohistochemical analysis, cryosections were initially rehydrated, and antigen retrieval was carried out by proteinase K digestion for 10 min at RT. After washing in PBS, section blocking was performed

in 1% BSA in PBS for 30 min, and sections were incubated overnight at RT with primary antibodies, and diluted in antibody diluent Dako REAL^{TM}. Antibodies against collagen type I (ab34710, 1:800), collagen type II (II-4C11, 1:100) and aggrecan (969D4D11, 1:300) were used for the visualization of the ECM deposition. The next day, sections were washed in PBS, and incubated for 1 h at RT with the secondary antibodies: a donkey anti-mouse (Cy3, 1:500) and a goat anti-rabbit (Alexa Fluor 488, 1:400) secondary antibody were used. Finally, the sections were washed in PBS, and nuclei were stained with DAPI mounting medium ImmunoSelect®. Images were taken with a fluorescence microscope (Olympus BX51/DP71, Olympus, Hamburg, Germany).

2.2.11. Biochemical analyses

After 21 d of chondrogenic differentiation, the MSC-laden hydrogels were washed twice in PBS, and homogenized at 25 Hz for 5 min with a TissueLyser (Qiagen, Hilden, Germany). After homogenization, the constructs were digested with 3 U ml^{-1} papain for 16 h at 60 °C. The DNA quantification of hydrogel lysates was carried out with Hoechst 33258 DNA intercalating dye fluorometrically (GENios pro spectrofluorometer; Tecan, Crailsheim, Germany) at 340 nm and 465 nm, with salmon testes as the DNA standard [28]. The amount of GAG deposition was determined using dimethylmethylene blue assay. Quantification was carried out with a spectrophotometer (MRX microplate reader; Dynatech Laboratories, Chantilly, USA) at 525 nm, and bovine chondroitin sulfate as standard [29]. The hydroxyproline assay was adapted to a 96-well format, and its content was measured after acid hydrolysis and oxidation of hydroxyproline with chloramine T and visualization with p-dimethylamino-benzaldehyde. Quantification was carried out with a spectrophotometer at 570 nm and L-hydroxyproline as standard. The amount of the total collagen was calculated with a hydroxyproline to collagen ratio of 1:10 [30, 31].

2.2.12. 3D printing

Three-dimensionally (3D) printed constructs were prepared using a 3D Discovery robotic dispensing system (RegenHU, Villaz-St-Pierre, Switzerland). G codes were generated as a vector file with BioCAD software (RegenHU, Villaz-St-Pierre, Switzerland).

Two print-heads were used for double printing: PCL was extruded using a PH3 print-head (precision extrusion deposition print-head, screw based extruder, HM110EX) with an inner needle diameter of 0.25 mm, and a PH2 print-head (pneumatic driven print-head, DD135N) with an inner needle diameter of 0.33 mm was used to print the hydrogel precursor solution. The precursor solution was composed of 10 wt.% cross-linking polymers (HA-SH and P(AGE-*co*-G)), 0.05 wt.% I2959 and 1 wt.% additional high molecular weight HA as a thickener.

The PCL reservoir was heated up to 85 °C and the PCL temperature at the print-head during deposition was 93 °C. PCL was printed with an extrusion speed of 17.5 revs min^{-1}, 3 bar extrusion pressure and a collector plate speed of 5 mm s^{-1}. For the deposition of the precursor solution, a pressure of 1 bar and a dosing distance of 0.13 mm was applied. Alternate strands of PCL and precursor solution were printed in a 12 × 12 mm square with a layer height of 0.2 mm. First, a crosshatch layer of PCL was printed with precursor solution deposited in between the PCL strands. The next layers of the PCL and hydrogel solution were angled at 90° with respect to the previous, underlying layers. After the four layers were printed, the precursor solution was cross-linked with UV light (bluepoint 4; Dr Hoenle AG, Munich, Germany) for 8 s with an average intensity of 130 mW cm^{-2}. The produced 3D constructs were analyzed with a stereomicroscope (SteREO Discovery.V20; Carl Zeiss Microscopy, Jena, Germany).

To assess cell survival after printing, hMSCs (6.0×10^6 MSC ml^{-1}) were added to the precursor solution. The solution was printed with the print-head PH2 (pneumatic driven print-head DD135N) with an inner needle diameter of 0.33 mm and a pressure of 1 bar directly into cylindrical molds (6 mm in diameter, 1 mm in height). The obtained constructs were irradiated with UV light (bluepoint 4, Dr Hoenle AG; Munich, Germany) for 8 s.

2.2.13. Statistics

Statistic evaluation was conducted using SigmaPlot 12.5 software. Multiple groups were compared using one-way ANOVA with a Tukey post hoc test, and a comparison of two groups was done with Student's *t*-test. Significant differences are marked as follows: $^{*}(p < 0.05)$, $^{**}(p < 0.01)$ and $^{***}(p < 0.001)$.

3. Results

3.1. Polymer synthesis and characterization

In order to covalently integrate biofunctional HA via thiol-ene cross-linking into the bioink, we modified HA with thiol groups, so that allyl-functional poly (glycidol) (P(AGE-*co*-G)) can be used as a multifunctional cross-linker. The modification of HA was performed in a two-step reaction based on a previously published protocol [12]: first, a nucleophilic substitution of DTPH to the carbodiimide activated carboxylic acid of the HA was conducted, followed by the subsequent reduction of the disulfide bonds within the dithio propionic acid to free thiols with DTT (figure 1(a)). P(AGE-*co*-G) was also synthesized according to literature [10], starting with an anionic bulk polymerization of AGE and EEGE monomers with subsequent deprotection of the EEGE monomers to the corresponding alcohol groups (figure 1(b)). ^{1}H-NMR was used to assess the degree of modification

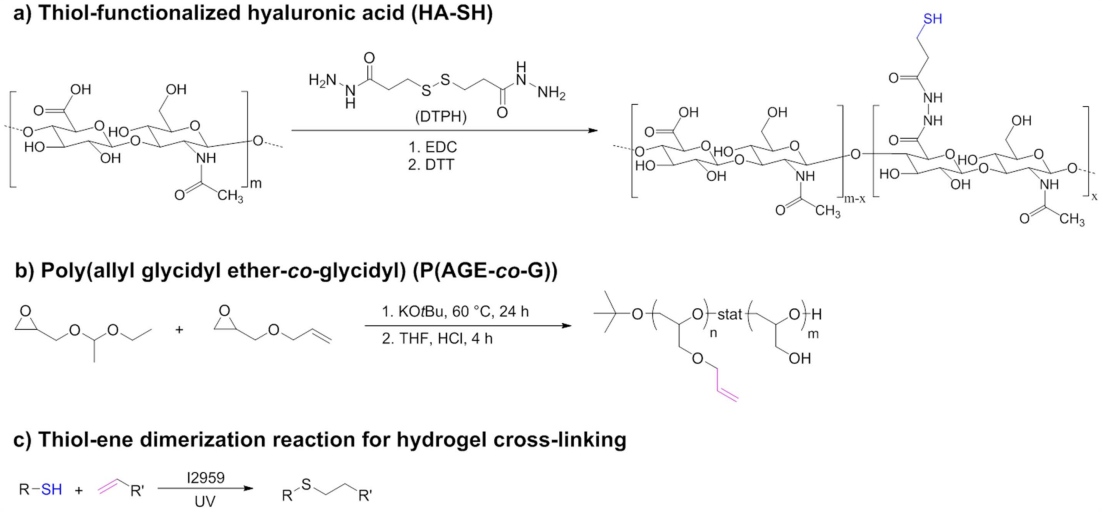

Figure 1. Schematic overview of polymer synthesis and thiol-ene UV reaction.

(DoM = amount of functional groups with respect to all monomer units in the backbone) in both polymers (SH and allyl, respectively) and revealed a SH-DoM of 41% of the original carboxyl functions for HA-SH and an allyl-DoM of 11% for P(AGE-*co*-G). Molecular weights were determined by GPC measurements relative to PEG standards and revealed a M_n of HA-SH of 7300 Da and a M_n of P(AGE-*co*-G) of 1500 Da.

3.2. Hydrogel formation

We then used these precursors for hydrogel formation via light-initiated radical thiol-ene coupling. This reaction is a selective dimerization reaction, in which thiols react with C–C double bonds to a thioether bridge between the educts (figure 1(c)). We used the photoinitiator I2959, which is activated by UV light (365 nm), to cross-link the synthetic polymer P(AGE-*co*-G) with the natural polymer HA-SH to a stable hybrid hydrogel. For physicochemical characterization, the hydrogels were examined with respect to their mechanical and swelling properties. For this study, two different hydrogel systems were prepared: one system with 10 wt.% cross-linkable polymers (HA-SH and P(AGE-*co*-G)) alone and the other system with the same polymers and additional high molecular weight HA (1.36 MDa; 1 wt.%), with the additional HA not being involved in the cross-linking reaction. For mechanical testing, the two different precursor solutions were dispensed into cylindrical molds (6 mm in diameter, 2 mm in height) and irradiated with UV light for 10 min. The Young's modulus of the resulting hydrogels was measured with a dynamic mechanical testing machine after 24 h swelling in PBS (figure 2(a)). The value of the Young's modulus for the system without additional high molecular weight HA was 66.3 ± 15.3 kPa and thus slightly higher than the Young's modulus for the hydrogels with additional physically incorporated HA (51.6 ± 13.7 kPa). After the mechanical testing, the hydrogels were dried and the SR was calculated (figure 2(b)). The SR for the hydrogels with additional HA was slightly higher (21.1 ± 2.4) than the SR for the gels without HA (15.7 ± 1), indicating weaker gel networks.

To further examine the swelling behavior of the hydrogels, the swelling profiles of cylindrical hydrogels were recorded over five weeks. Triplicates of the hydrogels were swollen in PBS at 37 °C and weighed at specific time points (figures 2(c)–(d)). Without additional HA in the formulation, the gels swelled within 1 h up to 140 ± 4.6% of their initial weight, and reached a swelling equilibrium of 122 ± 3.8% after 24 h (figure 2(a)). With the additional HA, the gels exhibited significantly stronger initial swelling up to 187 ± 17.3% of their initial weight after 1 h (figure 2(b)) but also showed a stronger decrease in swelling afterwards to reach equilibrium conditions at 135 ± 5.8% of the initial weight after 24 h. For both types of gels, the changes in swelling after 24 h were not pronounced over the subsequent five weeks.

3.3. Chondrogenic differentiation of hMSCs and eMSCs

In order to assess the cytocompatibility of the hybrid hydrogels, a live/dead assay was performed to estimate cell viability. Representative images for eMSC and hMSC are shown after day 2 and day 21 of chondrogenic differentiation (figure 3(a)). For eMSC, the staining of cytoplasm with calcein–AM showed the formation of larger cell aggregates and a more stretched cell shape after day 21, while hMSC aggregates appeared smaller and more rounded. Considering the viability, the cells from both species revealed good viability on day 2 with an increase of dead cells until day 21, but without large differences between the species. Additionally, the supplementation of the basic hydrogel formulation (P(AGE-*co*-G) + HA-SH) with

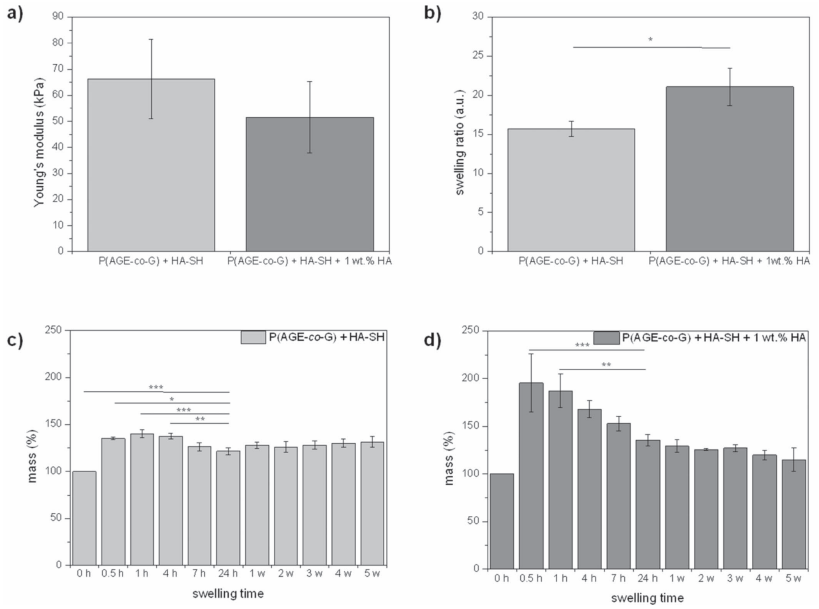

Figure 2. Mechanical properties and swelling data of the two investigated hydrogel systems: 10 wt.% polymer amount (P(AGE-*co*-G) and HA-SH) with and without additional HA (1 wt.%, 1.36 MDa). (a) Young's modulus, (b) SR after 24 h incubation in PBS, (c) and (d) swelling profile of hydrogels in PBS at 37 °C over five weeks.

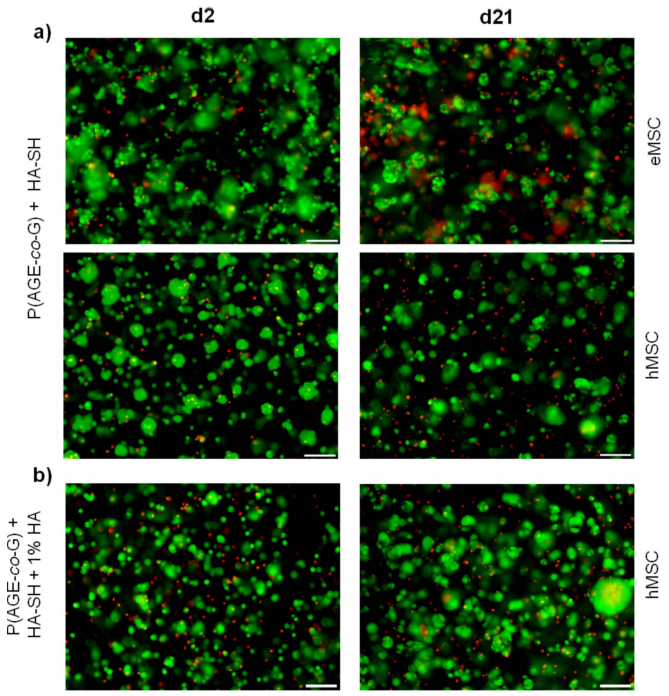

Figure 3. (a) Cell viability of *in vitro* cultured eMSCs and hMSCs embedded in hydrogels (P(AGE-*co*-G) + HA-SH) undergoing chondrogenic differentiation after day 2 and day 21, and (b) for hMSCs in P(AGE-co-G) + HA-SH with an additional 1 wt.% HA. Live/dead assay shows viable cells (green), labeled with calcein–AM, and dead cells (red), labeled with EthD-III. Scale bars represent 100 μm.

1 wt.% HA did not appear to negatively affect the hMSC viability (figure 3(b)).

Both hydrogel formulations supported the formation of cartilage-specific ECM by the encapsulated MSCs. The quantification of GAG and collagen amounts normalized to the contained DNA amount showed that abundant ECM components were produced. Thereby, the addition of 1 wt.% HA appeared to slightly reduce the GAG and collagen production of hMSCs in comparison with cells embedded in hydrogels without additional high molecular weight HA (table 1).

GAG staining with safranin O revealed that the deposition of proteoglycans was limited to pericellular

Table 1. Glycosaminoglycans per DNA (GAG/DNA) and collagen per DNA (collagen/DNA) for MSCs embedded in hybrid hydrogels (P(AGE-*co*-G) + HA-SH) and in P(AGE-*co*-G) + HA-SH with additional 1 wt.% HA ($n = 3$).

	P(AGE-*co*-G) + HA-SH		P(AGE-*co*-G) + HA-SH + 1% HA
	eMSC	hMSC	hMSC
GAG/DNA (μg/μg)	29.3 ± 1.0	34.2 ± 1.2	27.0 ± 5.8
Collagen/DNA (μg/μg)	18.5 ± 3.0	15.8 ± 0.6	11.9 ± 0.7

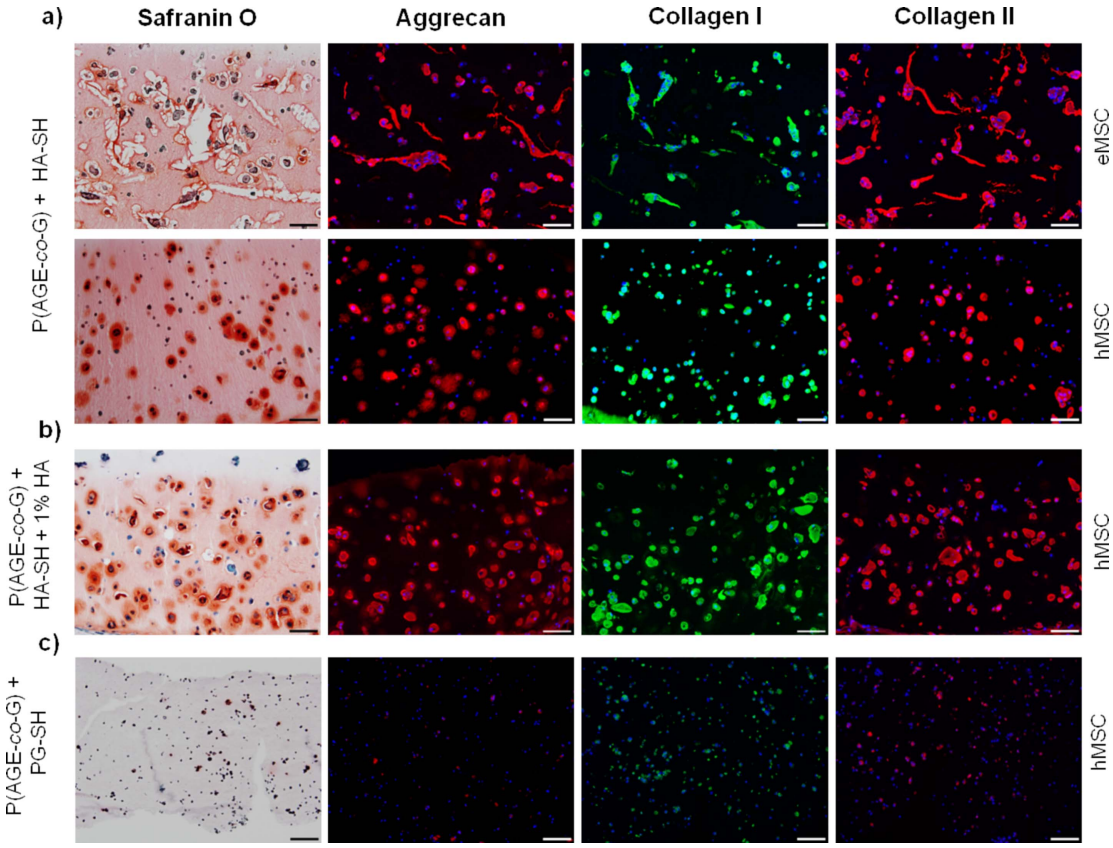

Figure 4. Histology and immunohistochemistry of (a) eMSCs and hMSCs embedded in hybrid hydrogels (P(AGE-*co*-G) + HA-SH), and (b) hMSCs embedded in P(AGE-co-G) + HA-SH with additional 1 wt.% HA; (c) in contrast, histology and immunohistochemistry of hMSCs embedded in pure synthetic hydrogel (P(AGE-*co*-G) + PG-SH; 15 wt.% polymer amount), in both cases after day 21 of chondrogenic differentiation *in vitro*. Cryosections were stained for the deposition of glycosaminoglycans with safranin O and aggrecan (red), collagen I (green) or collagen II (red) to visualize ECM production. Nuclei were labeled blue with DAPI; scale bars represent 100 μm.

regions after 21 d in cell-laden hydrogels (figure 4(a)). In addition, immunohistochemical (IHC) staining for the unspecific collagen type I and the cartilage-specific ECM molecules aggrecan and collagen type II showed similar patterns of specific ECM distribution, which were also more restricted to distinct areas in close proximity to the cell nuclei (figure 4(a)). Here, the addition of 1 wt.% HA led to a similar distribution of ECM components throughout the gel (figure 4(b)); however, the distribution of cells was more uneven in comparison to cells encapsulated in hydrogels consisting of the basic formulation (shown in figure S1, available online at stacks.iop.org/BF/9/044108/mmedia).

In order to demonstrate the effect of HA as a bioactive gel component, hMSCs were also embedded in a pure synthetic hydrogel (P(AGE-*co*-G) + PG-SH) and cultured in the same chondrogenic medium for 21 d. In the pure PG system [10], cross-linking occurs just between the allyl groups of the P(AGE-*co*-G) with the thiol-function of thiol-modified polyglycidol without the presence of HA. hMSCs incorporated in this pure synthetic hydrogel, without the supportive background of HA, clearly produced lower amounts of GAG, as shown in safranin O staining and IHC for aggrecan. The deposition of collagen type I and collagen type II was also considerably lower and restricted to pericellular regions (figure 4(c)). The differences in the distances of the visible cell nuclei compared to hybrid hydrogels (figure 4(a)) resulted from a strong shrinking of the pure PG hydrogels during the embedding process for cryosectioning (figure 4(c)).

3.4. 3D double printing and cell printing

First we evaluated whether the hydrogels could be printed via dispense plotting without support structures. Since the precursor solution alone could not be printed with adequate shape fidelity due to its low viscosity, we added unmodified HA (1.36 MDa) as a thickener in increasing amounts, and, with an addition of 2.5 wt.% HA, we obtained constructs with high shape fidelity by merely printing the gels (figure S2).

We then focused on double printing of the gels with PCL, as this is a well-accepted strategy for cartilage due to the beneficial compromise between the bioactive component of the gels and the mechanical strength provided by the PCL for mimicking this load bearing tissue. Hence, a hydrogel solution (10 wt.% polymer amount) with an increasing amount of additional unmodified HA as a thickener was double printed together with PCL with the aim of achieving stable 3D constructs for cell culture. Firstly, a PCL layer was printed, followed by printing the hydrogel precursor solution in between the PCL strands. Subsequent layers were printed at a 90° angle with respect to the previous layer. After printing four layers, the construct was UV irradiated for 8 s and the hydrogel solution was cross-linked. Double printing with 0.5 wt.% additional HA led to a spreading of the hydrogel and yielded soaked PCL layers, which prevented a good attachment of the subsequently printed PCL layer, and hence an overall weakened construct (figure S3). With the addition of a larger amount of HA (1 wt.% and 2.5 wt.%) it was possible to print constructs with a high shape fidelity (figure 5(a) for 1 wt.% and figure S3 for 2.5 wt.%, respectively). At this point it is important to recall that already the addition of 1 wt.% high molecular weight HA resulted in a slightly less robust chondrogenic differentiation of embedded hMSCs in comparison to hydrogels without additional HA (table 1). Therefore, double printing with PCL and the precursor solution with 1 wt.% HA appeared as the best compromise between optimal chondrogenic differentiation, chemical stability and mechanical stiffness.

Accordingly, the formulation with 1 wt.% supplemented HA was used to study the effect of printing on cells and accordingly the suitability of the bioink. hMSCs were added to the precursor solution, printed into cylindrical molds and cross-linked for 8 s. The live/dead staining of hMSCs after day 2 and day 21 of *in vitro* culturing showed high cell survival after the printing process (figure 5(b)). hMSCs appeared to be unharmed by the printing process and the resulting pictures of the live/dead assay were comparable to the results for the merely cast gels.

4. Discussion

In this study, we present a thiol-ene cross-linked hydrogel system based on the combination of a synthetic polymeric cross-linker and a modified natural polymer as a bioink. Our hydrogel system consists of an allyl-functionalized PG cross-linker and thiol-functionalized HA as a bioactive material. HA is a major component of the ECM and is utilized in hydrogels in many tissue engineering approaches [11–15]. Furthermore, the three different functional groups of HA, primary and secondary alcohol, the N-acetyl group and the carboxylic acid, allow quite a flexible modification, and thus the flexible use of functionalized HA in chemical cross-linking approaches [11]. Herein, we functionalized HA with thiols via the hydrazide formation with the carboxylic acid using DTPH and a subsequent reduction with DTT (figure 1(a)). Thiol-functionalized HA was successfully synthesized with a DoM of 41% of the carboxylic acid functions. The synthetic polymer cross-linker used in our hydrogel system is linear P(AGE-*co*-G). PGs are hydrophilic and biocompatible polymers, which can be obtained via anionic polymerization [8, 32]. Linear derivatives of PG are synthesized using accordingly protected glycidol monomers, such as, for example, acetal protected EEGE [9, 10]. In contrast to the most often used PEG, PG bears an alcohol group at every monomer unit and can therefore be functionalized in multiple and different ways [7]. Most easily this can be achieved via *co*polymerization of EEGE with other monomers such as AGE, thus introducing different functional groups, in the case of AGE allyl groups, into the polymer, which are in this case randomly distributed along the backbone. For our hydrogel system, we used P(AGE-*co*-G) with an allyl-functionality of 11% (figure 1(b)).

Using these polymers, hydrogels with 10 wt.% polymer concentration were prepared and their mechanical as well as swelling behavior was examined (figure 2). Two different systems were produced, one without and one with 1 wt.% additional, non-cross-linkable HA. The additional HA was added to the system in order to increase the viscosity of the precursor solution, which is ultimately necessary for 3D printing. Comparison of the two different gel systems showed that the system with additional HA was slightly less stiff and had a higher SR than the system without additional HA (figures 2(a)–(b)). The Young's modulus of the hybrid gels was 66.3 kPa without additional HA and 51.6 kPa with additional HA, and thus lower than the modulus of a pure PG-based hydrogel system, which was previously shown to have a value of 83.0 kPa [10]. The mechanical stiffness of the hydrogels provides information about the density of the hydrogel network and can be varied by different parameters, such as the polymer amount or hydrogel composition [10, 15, 33, 34]. A less dense network is in accordance with a lower Young's modulus, so that we conclude that the addition of an HA thickener disturbs the cross-linking of the gel precursors. The measured SR is in line with the calculated Young's modulus of the two different systems (figure 2(b)). Because of the

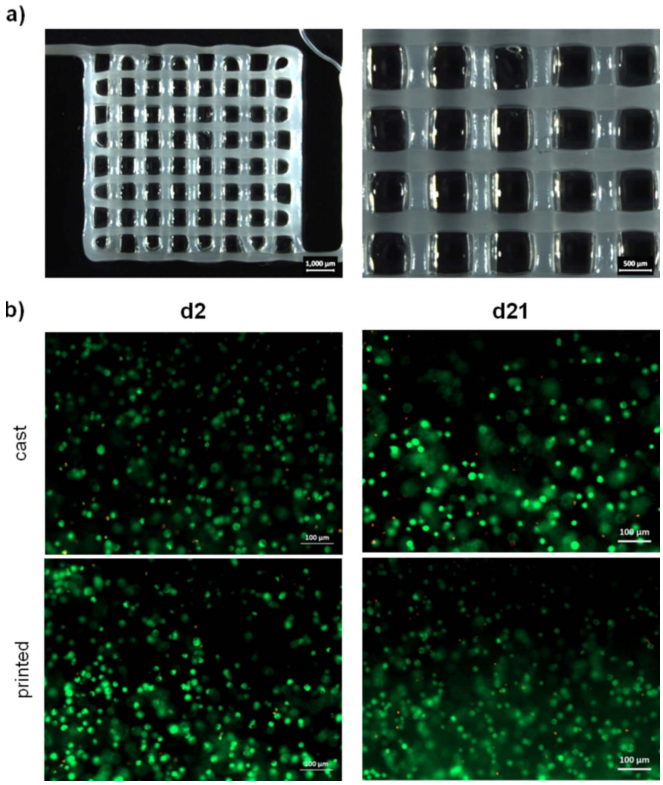

Figure 5. (a) 3D double printed construct with alternate strands of PCL and precursor solution (10 wt.% cross-linkable polymers, 0.05 wt.% I2959 and 1 wt.% additional HA); top view of a four-layer construct, layer height 0.2 mm and strand-to-strand distance of 1.0 mm; and (b) cell viability of *in vitro* cultured hMSCs embedded in hydrogels (P(AGE-*co*-G) + HA-SH + 1 wt.% HA). Live/dead staining of 3D printed hMSC after day 2 and day 21. Live/dead assay shows viable cells (green), labeled with calcein–AM, and dead cells (red), labeled with EthD-III. Scale bars represent 100 μm.

looser network, the hydrogel with additional HA can absorb more water than the hydrogel with a denser network. While this effect was most pronounced after 1 h, both gels approached a similar equilibrium swelling state at around 122% (without HA) and 135% (with additional HA), respectively, after 24 h, which did not exhibit any further pronounced changes over five weeks.

In order to prove the suitability of the proposed hydrogel formulation for the chondrogenesis of MSCs, MSCs from two different species—human and equine origin—were encapsulated within the hydrogels. Concerning viability, the scaffold material showed, for both hydrogel formulations and species, no significant differences (figure 3). Furthermore, the MSCs produced substantial amounts of cartilaginous ECM, as shown by the quantification of GAG and collagen (table 1). In contrast, the MSCs embedded in a pure PG synthetic hydrogel showed just very weak staining for GAG, aggrecan and collagen type II. Since PEG is known for its bioinert character [35], and PG is a structural analogue to PEG [7], the poor deposition of cellular-produced ECM molecules, and thus the low yield of chondrogenesis in the pure PG gels, was expected, despite the addition of TGF-β1 to the medium. However, the substitution of the bioinert PG-SH with HA-SH in the hydrogel formulation resulted in a significantly stronger staining for GAG, aggrecan and collagen type II and an overall improved chondrogenesis (figure 4). The analysis of MSC chondrogenesis in pure PEG gels compared to MeHA gels clearly demonstrated the advantages of HA incorporation [22], as we were also able to demonstrate when comparing pure PG gels with HA-SH gels (figure 4). However, the addition of 1 wt.% high molecular HA appeared to negatively influence hMSC chondrogenesis (table 1). This should be taken into account when formulations are optimized for printing, and in our case, the supplementation with high molecular weight HA for printabiliy was kept to a minimum.

Despite the significant positive effect of HA on MSC chondrogenesis, staining for GAG with safranin O or by IHC for aggrecan and collagen type II exhibited for both species a rather pericellular deposition of cartilage-specific ECM molecules after 21 d of *in vitro* chondrogenesis (figure 4(a)). This restricted accumulation of ECM molecules has been reported in several cases for MeHA gel systems and was shown to be dependent on the achieved macromer density [22, 36, 37]. Since we also observed a more pericellular deposition, one solution might be to decrease the macromer density, but this would directly affect the printing properties of the developed hydrogel, and is therefore not the first option. The additional incorporation of MMP-sensitive peptides in the cross-linking backbone of hydrogels has proven to be a practical

and effective approach to overcome this issue and achieve a more even distribution of a cellular-produced matrix in many different hydrogel systems [38–40]. This mechanism could be included in our set up by the introduction of MMP-cleavable peptides in the PG cross-linkers, which is a promising strategy for future experiments. Taken together, we demonstrate in this study the principle suitability of this basic hybrid bioink for MSC chondrogenesis of two different species.

In the literature, hydrogel solutions are most commonly increased in concentration to yield more viscous solutions and thereby denser and stiffer hydrogel networks for 3D printing [41]. As discussed above, this is no alternative here, since increased hydrogel stiffness not only increases the viscosity of the solutions but also leads to inhibited cell growth, migration and differentiation [41]. In order to balance the printability and biological efficacy of a hydrogel solution, many researchers try to improve the overall material properties by including mechanical supports using other biodegradable fibers or other structures composed of stable thermoplastics [42] or alternative mechanically stiff hydrogels [5]. Most notably, the inclusion of additional PCL strands as a structural support scaffold has been widely used for articular cartilage biofabrication [43].

For the best performance, we combined both strategies: by the addition of a small amount (1 wt.%) of high molecular HA, the viscosity of the precursor solution could be slightly increased without influencing hMSC survival (figure 3), and by double printing with PCL, we achieved robust scaffolds with a high shape fidelity (figure 5). The hydrogel is here supported by thermoplastics and thus can be printed even with lower viscosities. Furthermore, we showed that the hMSCs successfully survived the printing process and showed good cell survival after 21 d in culture. As discussed above, the addition of high molecular weight HA decreased the chondrogenic potential to a certain extent, and, therefore, the amount of HA should be kept as low as possible. Moreover, surrogates for HA as a thickener or alternative methods completely omitting HA as a thickener appear desirable.

The mechanical properties of double printed scaffolds depend strongly on the stiffness of the thermoplastic, which is significantly higher compared to hydrogel-only constructs [24]. This effect was previously shown for other hydrogel systems such as alginate [24]. It was demonstrated that alginate/PCL double printed constructs have a comparable stiffness to PCL-only constructs. By using the double printing technique, combining a thermoplastic with a hydrogel opens up the use of different hydrogel systems in bioprinting, which are not printable without the supporting structure of PCL.

5. Conclusion

In this study, we introduced a hydrogel system based on thiol-ene clickable PGs and bioactive immobilized HAs as a bioink. First, the two functionalized polymers were synthesized and analyzed via ^{1}H-NMR and GPC measurements. With those polymers, we produced two different hydrogel systems with and without additional high molecular weight HA and measured the stiffness, the SRs and the swelling profiles of the two hydrogel systems. Cell studies with MSCs from different species showed the supporting potential of the immobilized HA for chondrogenic differentiation in both systems. Furthermore, we could show that cells embedded in the hydrogel solutions were printable without being harmed. With the use of the double printing technique, we produced robust hydrogel-containing scaffolds mechanically supported by PCL strands. Double printing with thermoplastics accordingly enabled less viscous hydrogel solutions to be printed, thus opening up the possibility of printing a huge range of different hydrogels, which are yet not printable without a supporting structure.

Acknowledgments

The research leading to these results has received funding from the European Union's Seventh Framework Programme (FP7/2007–2013) under Grant Agreement no. 309962 (Project HydroZONES) and from the Interdisciplinary Center for Clinical Research Würzburg (Project Number D-219).

ORCID iDs

Jos Malda https://orcid.org/0000-0002-9241-7676
Jürgen Groll https://orcid.org/0000-0003-3167-8466

References

[1] Groll J *et al* 2016 Biofabrication: reappraising the definition in an evolving field *Biofabrication* **13001** 1–6
[2] Mouser V H M, Abbadessa A, Levato R, Hennink W E, Vermonden T, Gawlitta D and Malda J 2017 Development of a thermosensitive HAMA-containing bio-ink for the fabrication of composite cartilage repair constructs *Biofabrication* **9** 15026
[3] Daly A C, Critchley S E, Rencsok E M and Kelly D J 2016 A comparison of different bioinks for 3D bioprinting of fibrocartilage and hyaline cartilage *Biofabrication* **8** 45002
[4] Shim J-H *et al* 2016 Three-dimensional bioprinting of multilayered constructs containing human mesenchymal stromal cells for osteochondral tissue regeneration in the rabbit knee joint *Biofabrication* **8** 14102
[5] Melchels F P W, Blokzijl M M, Levato R, Peiffer Q C, de Ruijter M, Hennink W E, Vermonden T and Malda J 2016 Hydrogel-based reinforcement of 3D bioprinted constructs *Biofabrication* **8** 35004
[6] O'Connell C D *et al* 2016 Development of the Biopen: a handheld device for surgical printing of adipose stem cells at a chondral wound site *Biofabrication* **8** 15019

[7] Thomas A, Müller S S and Frey H 2014 Beyond poly(ethylene glycol): linear polyglycerol as a multifunctional polyether for biomedical and pharmaceutical applications *Biomacromolecules* **15** 1935–54
[8] Dworak A, Slomokowski S, Basinska T, Gosecka M, Walach W and Trzebicka B 2013 Polyglycidol—how is it synthesized and what is it used for? *Polimery* **58** 641–9
[9] Erberich M, Keul H and Möller M 2007 Polyglycidols with two orthogonal protective groups: preparation, selective deprotection, and functionalization *Macromolecules* **40** 3070–9
[10] Stichler S, Jungst T, Schamel M, Zilkowski I, Kuhlmann M, Böck T, Blunk T, Teßmar J and Groll J 2017 Thiol-ene clickable poly(glycidol) hydrogels for biofabrication *Ann. Biomed. Eng.* **45** 273–85
[11] Burdick J A and Prestwich G D 2011 Hyaluronic acid hydrogels for biomedical applications *Adv. Mater.* **23** 41–56
[12] Shu X Z, Liu Y, Luo Y, Roberts M C and Prestwich G D 2002 Disulfide cross-linked hyaluronan hydrogels *Biomacromolecules* **3** 1304–11
[13] Shu X Z, Liu Y, Palumbo F and Prestwich G D 2003 Disulfide-crosslinked hyaluronan-gelatin hydrogel films: a covalent mimic of the extracellular matrix for *in vitro* cell growth *Biomaterials* **24** 3825–34
[14] Crescenzi V, Cornelio L, Di Meo C, Nardecchia S and Lamanna R 2007 Novel hydrogels via click chemistry: synthesis and potential biomedical applications *Biomacromolecules* **8** 1844–50
[15] Lee K Y and Mooney D J 2001 Hydrogels for tissue engineering *Chem. Rev.* **101** 1869–80
[16] Yang J, Zhang Y S, Yue K and Khademhosseini A 2017 Cell-laden hydrogels for osteochondral and cartilage tissue engineering *Acta Biomater.* **57** 1–25
[17] Mouser V H M, Levato R, Bonassar L J, DLima D D, Grande D A, Klein T J, Saris D B F, Zenobi-Wong M, Gawlitta D and Malda J 2017 Three-dimensional bioprinting and its potential in the field of articular cartilage regeneration *Cartilage* **8** 327–40
[18] Zhu H, Mitsuhashi N, Klein A, Barsky L W, Weinberg K, Barr M L, Demetriou A and Wu G D 2006 The role of the hyaluronan receptor CD44 in mesenchymal stem cell migration in the extracellular matrix *Stem. Cells* **24** 928–35
[19] Hardwick C, Hoare K, Owens R, Hohn H P, Hook M, Moore D, Cripps V, Austen L, Nance D M and Turley E A 1992 Molecular cloning of a novel hyaluronan receptor that mediates tumor cell motility *J. Cell Biol.* **117** 1343–50
[20] Solis M A, Chen Y H, Wong T Y, Bittencourt V Z, Lin Y C and Huang L L H 2012 Hyaluronan regulates cell behavior: a potential niche matrix for stem cells *Biochem. Res. Int.* **2012** 346972
[21] Nettles D L, Vail T P, Morgan M T, Grinstaff M W and Setton L A 2004 Photocrosslinkable hyaluronan as a scaffold for articular cartilage repair *Ann. Biomed. Eng.* **32** 391–7
[22] Chung C and Burdick J A 2009 Influence of three-dimensional hyaluronic acid microenvironments on mesenchymal stem cell chondrogenesis *Tissue Eng.* A **15** 243–54
[23] Wu S C, Chang J K, Wang C K, Wang G J and Ho M L 2010 Enhancement of chondrogenesis of human adipose derived stem cells in a hyaluronan-enriched microenvironment *Biomaterials* **31** 631–40
[24] Schuurman W, Khristov V, Pot M W, van Weeren P R, Dhert W J A and Malda J 2011 Bioprinting of hybrid tissue constructs with tailorable mechanical properties *Biofabrication* **3** 21001
[25] Visser J, Gawlitta D, Benders K E M, Toma S M H, Pouran B, van Weeren P R, Dhert W J A and Malda J 2015 Endochondral bone formation in gelatin methacrylamide hydrogel with embedded cartilage-derived matrix particles *Biomaterials* **37** 174–82
[26] Ruan J-L, Tulloch N L, Muskheli V, Genova E E, Mariner P D, Anseth K S and Murry C E 2013 An improved cryosection method for polyethylene glycol hydrogels used in tissue engineering *Tissue Eng.* C **19** 794–801
[27] Martin I, Obradovic B, Freed L E and Vunjak-Novakovic G 1999 Method for quantitative analysis of glycosaminoglycan distribution in cultured natural and engineered cartilage *Ann. Biomed. Eng.* **27** 656–62
[28] Kim Y-J, Sah R L Y, Doong J-Y H and Grodzinsky A J 1988 Fluorometric assay of DNA in cartilage explants using Hoechst 33258 *Anal. Biochem.* **174** 168–76
[29] Farndale R W, Buttle D J and Barrett A J 1986 Improved quantitation and discrimination of sulphated glycosaminoglycans by use of dimethylmethylene blue *BBA—Gen. Subj.* **883** 173–7
[30] Woessner J F 1961 The determination of hydroxyproline in tissue and protein samples containing small proportions of this imino acid *Arch. Biochem. Biophys.* **93** 440–7
[31] Hollander A P, Heathfield T F, Webber C, Iwata Y, Bourne R, Rorabeck C and Poole A R 1994 Increased damage to type II collagen in osteoarthritic articular cartilage detected by a new immunoassay *J. Clin. Invest.* **93** 1722–32
[32] Kainthan R K, Janzen J, Levin E, Devine D V and Brooks D E 2006 Biocompatibility testing of branched and linear polyglycidol *Biomacromolecules* **7** 703–9
[33] Meyer U, Meyer T, Handschel J and Wiesmann H P (ed) 2009 *Fundamentals of Tissue Engineering and Regenerative Medicine* (Berlin: Springer) pp 495–517
[34] Abbadessa A, Mouser V H M, Blokzijl M M, Gawlitta D, Dhert W J A, Hennink W E, Malda J and Vermonden T 2016 A synthetic thermosensitive hydrogel for cartilage bioprinting and its biofunctionalization with polysaccharides *Biomacromolecules* **17** 2137–47
[35] Zhu J 2010 Bioactive modification of poly(ethylene glycol) hydrogels for tissue engineering *Biomaterials* **31** 4639–56
[36] Erickson I E, Huang A H, Sengupta S, Kestle S, Burdick J A and Mauck R L 2009 Macromer density influences mesenchymal stem cell chondrogenesis and maturation in photocrosslinked hyaluronic acid hydrogels *Osteoarthr. Cartil.* **17** 1639–48
[37] Bian L, Hou C, Tous E, Rai R, Mauck R L and Burdick J A 2013 The influence of hyaluronic acid hydrogel crosslinking density and macromolecular diffusivity on human MSC chondrogenesis and hypertrophy *Biomaterials* **34** 413–21
[38] Bahney C S, Hsu C-W, Yoo J U, West J L and Johnstone B 2011 A bioresponsive hydrogel tuned to chondrogenesis of human mesenchymal stem cells *FASEB J.* **25** 1486–96
[39] Feng Q, Zhu M, Wei K and Bian L 2014 Cell-mediated degradation regulates human mesenchymal stem cell chondrogenesis and hypertrophy in MMP-sensitive hyaluronic acid hydrogels *PLoS One* **9** e99587
[40] Mhanna R, Öztürk E, Vallmajo-Martin Q, Millan C, Müller M and Zenobi-Wong M 2014 GFOGER-modified MMP-sensitive polyethylene glycol hydrogels induce chondrogenic differentiation of human mesenchymal stem cells *Tissue Eng.* A **20** 1165–74
[41] Malda J, Visser J, Melchels F P, Jüngst T, Hennink W E, Dhert W J A, Groll J and Hutmacher D W 2013 25th anniversary article: Engineering hydrogels for biofabrication *Adv. Mater.* **25** 5011–28
[42] Zhu J and Marchant R E 2011 Design properties of hydrogel tissue-engineering scaffolds *Expert Rev. Med. Devices* **8** 607–26
[43] Woodfield T B F, Malda J, de Wijn J, Péters F, Riesle J and van Blitterswijk C A 2004 Design of porous scaffolds for cartilage tissue engineering using a three-dimensional fiber-deposition technique *Biomaterials* **25** 4149–61